Table 2 Significant parameters applicable to low- and high-altitude tests

W,[a] lb	Parachute type	D_0, ft	Altitude, ft	M	q, psf	$\Delta q/\Delta t$, psf/sec (avg.)	m_a,[b] lb
280	Disk-gap-band	40.0	140,000	1.91	11.6	3.9[c]	0.007
221	Modified ringsail	31.2	122,500	1.39	11.0	4.6	0.006
240	Cross	30.0	136,000	1.57	9.7	2.8	0.003
394	Disk-gap-band	40.0	10,600	0.35	73.9	54.0	70.0
380	Modified ringsail	31.2	10,100	0.34	76.9	55.0	33.0
390	Cross	30.0	10,400	0.28	80.9	49.0	30.0
394	Cross	30.0	10,600	0.27	75.4	48.0	30.0

[a] Total descent system weight.

[b] Apparent mass m_a assumed equal to $\rho V/4$ (V = projected-area-hemisphere volume = $2A^{3/2}/3(\pi)^{1/2}$.

[c] Δq change in the interval between line stretch and peak load.

Discussion

Table 2 compares the parameters considered to be significant in affecting parachute performance for the tests to be discussed in this paper, that is, q, Mach number M, altitude, and system weight.

Probably the most significant difference in deployment characteristics between high- and low-altitude tests observed by onboard camera film is the effect of the "apparent mass" m_a at low altitude. For Table 2, m_a is assumed to be equal to $\rho V/4$, where ρ is the local air density and V is the volume of a hemisphere with a diameter equal to the projected diameter (two-thirds nominal diameter) of the parachute. This m_a is ~0.005 lb at high altitude and 30 to 70 lb at low altitude. (The weight of the parachute canopies was about 20 lb.) At low altitude, immediately after canopy inflation and rapid system deceleration, the canopy became significantly distorted, due to the effect of the mass of air in the wake not decelerating along with the flight system, which the authors refer to herein as an "apparent mass effect." This condition is sometimes called "over-inflation." The cross parachute was much less affected by this effect than the other two canopies.

The M's for the low-altitude tests had to be subsonic to avoid prohibitive loadings for the test canopies. For high-altitude tests with deployments above $M = 2$, the canopies opened to full inflation and then exhibited a partial inflation and a corresponding lower average drag than that exhibited at lower velocities. The dynamic pressure change with time ($\Delta q/\Delta t$ in Table 2) during inflation was essentially an order of magnitude less at high altitude, as compared to low altitude (2.5-5 psf/sec vs 48-55 psf/sec). At high altitudes, peak loading corresponded to first full inflation, while at low altitude, peak loading occurred prior to full inflation. Thus, when deploying essentially the same system at different altitudes, a significant load-alleviating effect is seen with decreasing altitude due to the larger velocity decay during inflation and, thus, for a given parachute system, deployment without structural damage can be initiated at a higher q at low altitude.

The test results presented have been from parachutes fabricated of cloth having a permeability range of 70 to 160 ft^3/min-ft^2 at a differential pressure of 0.5 in. of water. The effects of a wider range of cloth permeability (effective porosity) on opening and stability characteristics of parachutes over large altitude differences are, as yet, unknown. Some research on this effect appears warranted.

These low- and high-altitude data have been correlated nicely by Greene[6] to show that the opening distance of a parachute varies with M. Further analyses such as these may make it possible to conduct low-altitude drop tests and use the results to predict performance at high altitude. At the present time, it appears that the performance differences over large altitude increments are not sufficiently predictable to use this technique to advantage.

References

[1] Murrow, H. N. and McFall, J. C., "Summary of Experimental Results Obtained From the NASA Planetary Entry Parachute Program," *Proceedings of FTC-TR-69-11*, Air Force Flight Test Center, 1969; also *Journal of Spacecraft and Rockets*, Vol. 6, No. 5, May 1969, pp. 621-623.

[2] Preisser, J. S., Eckstrom, C. V., and Murrow, H. N., "Flight Test of a 31.2-Foot-Diameter Modified Ringsail Parachute Deployed at a Mach Number of 1.39 and a Dynamic Pressure of 11.0 Pounds Per Square Foot," TM X-1414, Aug. 1967, NASA.

[3] Preisser, J. S. and Eckstrom, C. V., "Flight Test of a 40-Foot-Nominal-Diameter Disk-Gap-Band Parachute Deployed at a Mach Number of 1.91 and a Dynamic Pressure of 11.6 Pounds Per Square Foot," TM X-1575, May 1968, NASA.

[4] Preisser, J. S. and Eckstrom, C. V., "Flight Test of a 30-Foot-Nominal-Diameter Cross Parachute Deployed at a Mach Number of 1.57 and a Dynamic Pressure of 9.7 Pounds Per Square Foot," TM X-1542, April 1968, NASA.

[5] "Performance of and Design Criteria for Deployable Aerodynamic Decelerators," ASD-TR-61-579, Dec. 1963, U.S. Air Force.

[6] Greene, G. C., "Opening Distance of a Parachute," *Journal of Spacecraft and Rockets*, Vol. 7, No. 1, Jan. 1970, pp. 98-100.

A 30-cm Mercury Ion Thruster Module

H. J. KING* AND R. L. POESCHEL†
Hughes Research Laboratories, Malibu, Calif.

IN an earlier paper,[1] the scaling and development of a SERT II thruster design to 30-cm diam was presented. This Note describes the optimization procedures and performance characteristics of the thruster system which has evolved during the ensuing period. A principal task was the selection of an ion optical system for operation at a specific impulse (I_{sp}) of 2750 sec. Several designs of conventional two-grid systems and single, dielectric-coated grid systems were evaluated experimentally, and a single grid system (having apertures of 0.2-cm diam on 0.25-cm center-to-center spacing in hexagonal array) was the best of the systems tested at that time. The next task was to optimize the thruster discharge chamber for operation at the 27 mlb thrust level.

The optimization effort drew heavily on the results of Bechtel[2] and communications with other NASA LeRC staff members. On the basis of this information, the only parameters which required modification were magnetic field strength and baffle size. Included in the optimization effort was the integration of a hollow cathode plasma bridge neutralizer, as well as several other components necessary to complete the thruster module, including a more durable thruster cathode, propellant electrical isolators and efficient propellant vaporizers. The complete thruster module was tested for 500 hr. All components performed well. With the exception of the dielectric grid all component lifetimes can be extrapolated to more than 10,000 hr. Although several reasons for the failure of the dielectric optics have been postulated (i.e., back-sputtered material from the beam collector, inhomo-

Presented as Paper 70-1099 at the AIAA 8th Electric Propulsion Conference, Stanford, Calif., August 31–September 2, 1970; submitted October 23, 1970; revision received December 18, 1970. Supported in part by NASA-Lewis Research Center.

* Head, Propulsion Technology Section. Associate Fellow AIAA.

† Senior Staff Engineer. Member AIAA.

Table 1 Development program goals

Specific impulse	I_{sp} = 2750 sec
Beam voltage	V_B = 1000 v
Beam current	I_B = 1.85 amp
Electrode lifetime	10^4 hr
Thruster diameter	30 cm
Thruster efficiency	64%

geneous dielectric coating, etc.), the cause and prevention of the observed dielectric coating failure have not yet been conclusive.

Ion Optical System Selection

The goals of this development program were as shown in Table 1.

The parameters considered in the design were size, shape, and number of apertures; accel-decel ratio (which defines the total acceleration voltage); electrode thickness; electrode spacing; method of mounting the electrodes; and methods of fabrication.[1,3] For a conventional two-grid ion optical system for operation at low I_{sp}, the principal problem is in maintaining structural integrity while decreasing grid spacing and screen thickness. In addition, it is difficult to maintain enough open area (>70% to maintain electrical efficiency) while increasing the number of apertures. After performing thermal and ion optical analyses, several designs were fabricated from molybdenum by match-drilling screen and accel electrodes, and the ion optical system was supported by 6 brackets mounted at the periphery and one center spacer. Six conventional systems (Table 2) were tested. The design of the dielectric-coated electrodes was more empirical in nature and proved to be more a fabrication technology development effort to obtain a uniform, void-free coating of suitable thickness without obstructing any of the apertures.

The molybdenum substrate is prepared by chemically milling the hexagonal hole pattern into it, then dishing it by power hammering. The coating is applied by spraying a series of thin (~0.01-in.) layers of mullite and glass frit in a water suspension on the electrode and firing each layer at approximately 1100°C in N_2. The glass-mullite mixture is refractory and does not change its shape when fired. It forms a porous, chalk-like coating which can be mechanically shaped after firing. This skeletal coating is then filled by coating with thin layers of glass which flows into the pores readily when fired at 1100°C. A glaze coat is then applied and fired.

Figure 1 illustrates the acceleration mechanism. Test data for several dielectric coated grids are shown in Table 2.

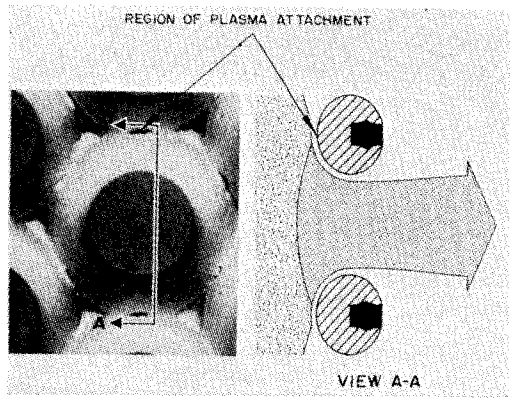

Fig. 1 Photograph of insulated ion optics after operation, showing plasma attachment.

The relationship between beam current I_B and total voltage V_I obeys Child's law within a factor determined by the position of the plasma boundary; this relationship may be referred to as the thruster perveance, $P_T = I_B/V_T^{3/2}$. The V_T that could safely be applied across the dielectric coating without danger of electrical breakdown was ~2000 v. During operation a typical operation point was V_B = 1000 v and V_{Accel} = −500 v, giving V_T = 1500 v, which provided a sufficient margin of safety for stable operation. The insulated electrode had adequate perveance under these conditions to extract and focus the 1.85 amp beam necessary to operate the thruster at 2.5 kw input power.

The upper limit to the total extraction voltage when using conventional two-grid extraction system is less well-defined, since with careful mechanical design, voltages of ten times the desired V_B (1 kv) can easily be sustained. For this study a maximum V_T of 3 kv was chosen rather arbitrarily to limit the beam divergence, which increases rapidly with accel-decel ratio. By reducing the screen electrode thickness to 0.020 in. and the interelectrode spacing to 0.025 in., it was possible to increase P_T to a point where a 1.85-amp beam may be extracted. Although no life tests were conducted with these particular ion optics, they should have a useful lifetime of the order of 10^4 hr. One disadvantage of this conventional grid system is that even with an open area of 72%, which is a practical mechanical limit, the over-all thruster efficiency is less than that when using the insulated optics by 8%.

Because of their improved efficiency and lighter weight but unknown lifetime limitations, the remainder of the optimization program was conducted with insulated optics.

Table 2 Summary of ion optical system performance

Test No.	V_+ kv	I_+ amp	V_- kv	I_- ma	V_D v	I_D amp	M^a amp (equiv.)	η_m, (%)	$\epsilon_I{}^b$ eV/ ion	Screen: Aperture diameter (cm)	Screen: Thick (cm)	Accelerator: Aperture diameter (cm)	Accelerator: Thick (cm)	Grid spacing (cm)	Open area (%)	$k = \frac{I_+{}^d}{V_T{}^{3/2}}$ amp/volt$^{3/2}$ × 10^{-5}
a) Conventional, two-grid ion optical systems																
1a	1.0	1.5	1.95	12	43	17	2.16	76	432	0.2	0.075	0.19	0.125	0.165	62	0.92
1b	1.0	1.56	1.9	20	35	18.2	2.2	71	415	0.2	0.075	0.19	0.125	0.115	62	0.92
2	1.0	1.44	2.0	14	39	12.7	1.62	91.5	347	0.2	0.045	0.19	0.125	0.115	62	0.92
3	2.7	1.6	1.0	16	33	10.2	1.88	88.5	212	0.40	0.075	0.32	0.27	0.100	72	0.76
4	1.0	1.9	1.52	50	41.5	14	2.31	80	314	0.20	0.045	0.19	0.125	0.064	62	1.50
5	1.0	1.89	2.0	23	37	10.6	2.10	88.5	210	0.40	0.045	0.32	0.27	0.064	72	1.22
6	1.4	1.75	2.0	13	37	11.4	1.94	89.3	243	0.40	0.045	0.32	0.27	0.081	72	1.10
b) Dielectric-coated, single-grid ion optical system[c]												$t_{coat(average)}$, cm				
I	1.0	1.79	0.77	30	47	9.8	2.14	85.5	257	0.2	0.05	0.055				2.4
II	1.0	1.59	0.64	40	35.4	9.8	2.01	86.5	218	0.2	0.05	0.055			footnote	2.4
III	1.0	1.87	0.5	63	37.2	12.5	2.15	88.2	249	0.2	0.05	0.070		N.A.	c	3.0
IV	1.0	1.904	0.4	50	40.9	8.6	2.06	93.4	190	0.2	0.05	0.075				3.5

[a] Propellant flow and utilization pertain to flow through discharge chamber only (does not include neutralizer).
[b] Ionization efficiency of discharge chamber.
[c] Geometric open area less than 50%, estimate effective transmission of the order of 85%.
[d] Effective perveance constant for thruster, $V_T = V_+ + |V_-|$.

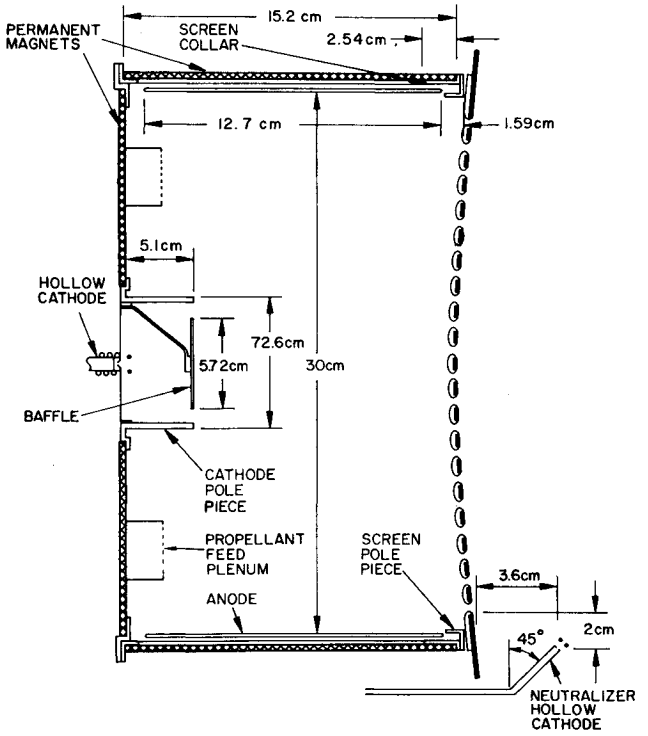

Fig. 2 30-cm-diam thruster optimized for operation at 2.5 kw power, 2750 sec specific impulse.

Discharge Chamber Development

The optimized thruster configuration (Fig. 2) differs only slightly from the one reported by Bechtel.[2] It makes use of both radial and axial bar magnets to create the desired magnetic field shape; whereas Bechtel's design has a broad screen collar to produce diverging magnetic lines of force. In addition, the baffle diameter is somewhat larger in order to maintain higher discharge voltage (38 v) at the higher thrust level desired in this program. Figure 3 shows the discharge chamber performance improvements which resulted from changing the baffle diameter and the number of axial magnets. Curve I represents the performance of the scaled SERT II thruster operated with a dielectric-coated grid at 1000-v net accelerating voltage. Curve II was obtained by increasing the baffle diameter from 5.1cm to 5.7cm. Curve III resulted from increasing the number of axial magnets from 13 to 15 (slight change in both field shape and magnitude). The improvement from III to IV is attributed to improved

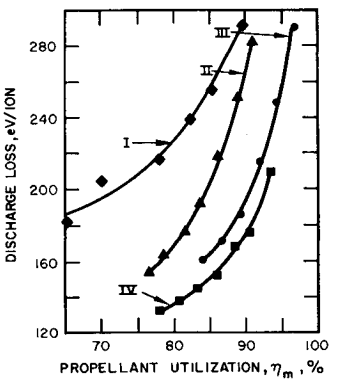

Fig. 3 Comparison of performance mapping for several stages of thruster development. I) 5.1-cm-diam baffle; II) 5.7-cm-diam baffle with improved mount; III) increase number of axial magnets from 13 to 15; IV) welded constructions, improved grid quality.

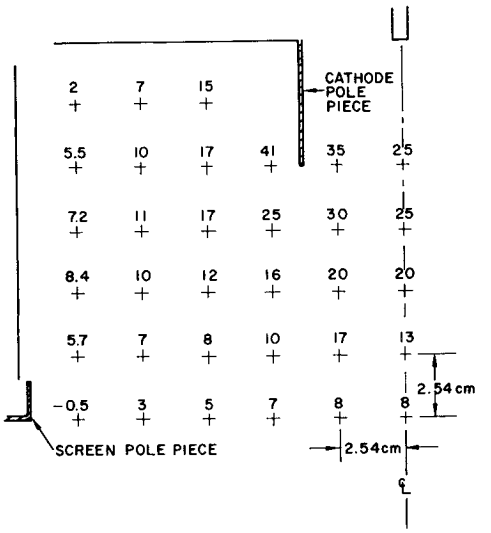

Fig. 4 Axial magnet field mapping for optimized magnetic configuration generated by 8 radial and 15 axial permanent magnets. Field values are in Tesla $\times 10^4$.

extraction grid fabrication technique. A map of the axial field strengths in the optimized discharge chamber is shown in Fig. 4.

Several components incorporated in this thruster module which bring it closer to flight status are the plasma bridge neutralizer, the propellant electrical isolator, and an advanced cathode orifice geometry. The plasma bridge neutralizer consists of a hollow cathode and keep-alive electrode, positioned downstream of the accelerator electrode to emit electrons into the beam. Several iterations were performed in changing the location and the pointing angle of the neutralizer cathode. The neutralizer hollow cathode must inject electrons into the ion beam with both a minimum voltage drop and a minimum of expellant. In addition, the charge exchange ions resulting from the Hg expellant which leaves the neutralizer (~2% of the total Hg flow) must not cause undue erosion on the downstream surface of the accelerator grid. The location and angle shown in Fig. 2 (3.6 cm downstream of the accelerator, 2 cm from the beam edge and making a 45° angle with the beam) proved to be satisfactory. All test results presented here were obtained with the neutralizer in this position.

The propellant electrical isolator permits the propellant vaporizers and propellant storage to be operated at ground potential (spacecraft potential). Separate propellant vaporizers and isolators were used for supplying Hg vapor to the thruster cathode and to the discharge chamber. The type of isolator developed by Hughes prevents breakdown of the Hg vapor at any pressure by using a number of gaps, across which the voltage remains below the Paschen minimum. This isolator (Fig. 5) can withstand up to 2.5 kv safely. Leakage at the design beam voltage (1 kv) is typically 3-5 μa.

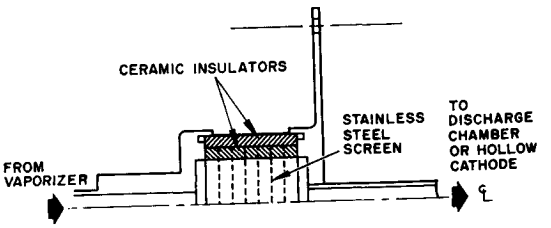

Fig. 5 Isolator assembly for 2 amp neutral vapor flow.

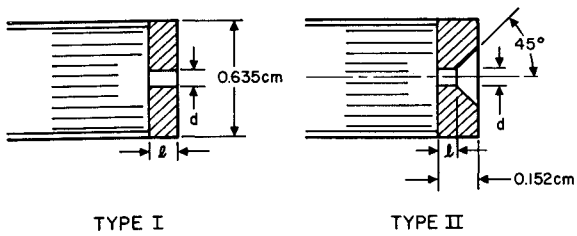

Fig. 6 Hollow cathode tip and orifice configurations.

At the outset of the program a hollow cathode configuration was required which could operate at 10-amp emission without severe erosion of the orifice. The initial design was of type I shown in Fig. 6 with $d = 0.038$ cm and $l = 0.152$ cm. It eroded rapidly during the first few hours of operation, after which the erosion rate reduced. Drawing on the results of Rawlin and Kerslake[4] and testing cathodes with variations in d and l, it was determined that initial erosion was proportional to the self-heated operating temperature, which increases with increasing l or decreasing d. Since the initial erosion usually has the form of a chamfering of the orifice, configuration II of Fig. 6 was chosen. It permits a short l without severely impairing the thermal conduction of heat from the orifice region (which always appears brighter than the rest of the cathode tip when viewed with a pyrometer). The values of l and d which displayed no initial erosion were $l = 0.051$ cm and $d = 0.076$.

Evaluation Testing

The 500-hr test was continuously manned, and data were recorded at half-hour intervals. A data summary is presented in Table 3. All components except the dielectric-coated accelerator grid performed extremely well. The plasma bridge neutralizer operated well with no indication of a change in its properties. The propellant electrical isolators showed no increase in leakage throughout the 500 hr. No erosion could be detected on the thruster hollow cathode orifice. Three accelerator grids had to be used to complete the 500-hr test period. The failure mode cannot be, at present, convincingly explained. Several investigations are under way to determine whether the failure problem is basic in nature, or the result of inadequate technological development in either the fabrication or testing procedures.

Table 3 500-hr test performance summary

Parameter	Total test[a] V, v	I, amp	P, w
Beam	1000	1.854	1854.0
Discharge	40.9	8.6	353.0
Accelerator[b]	405	0.050	70.2
Cathode and isolator heater	18.1	2.8	50.6
Neutralizer heater	5.0	2.9	14.5
Cathode keeper	8.0	0.28	2.2
Neutralizer keeper	9.7	0.22	2.1
Main vaporizer	3.6	2.4	8.6
Cathode vaporizer	2.3	2.0	4.6
Neutralizer vaporizer	1.5	1.1	1.6
Neutralizer coupling[c]	21.9	1.854	40.6
Total power		2,402.0 w	
Total losses		548.0 w	
Electrical efficiency		77.1%	
Mass efficiency		90.0%	
Total efficiency		69.4%	
Thrust		27.0 mlb	
I_{sp}		2,846 sec	
Power/thrust		89 w/mlb	
ev/ion		190	
Main flow rate		1.02 cm³/hr	
Cathode flow rate		0.077 cm³/hr	
Neutralizer flow rate		0.042 cm³/hr	

[a] Test conducted in three segments using different ion optical systems.
[b] Accel power is computed as $I_{accel} \times V_{total}$.
[c] Neut. coupling volt = thruster floating potential plus estimated beam potential of 12 v.

Conclusions

An engineering model of a 30-cm-diam thruster module has been developed for operation at 2-½-kw power level and I_{sp} of 2850 sec. Extensive testing has shown it to possess the performance characteristics suitable for a solar-electric-propulsion, deep-space mission. The performance characteristics here should represent state-of-the-art for a thruster module of this size.

References

[1] King, H. J., Poeschel, R. L., and Ward, J. W., "A 30 cm, Low Specific Impulse, Hollow Cathode Mercury Thruster," *Journal of Spacecraft and Rockets*, Vol. 7, No. 4, April 1970, pp. 416–421.

[2] Bechtel, R. T., "Performance and Control of a 30 cm Diameter Low Impulse Kaufman Thruster," *Journal of Spacecraft and Rockets*, Vol. 7, No. 1, Jan. 1970, pp. 21–25.

[3] King, H. J. and Poeschel, R. L., "Low Specific Impulse Ion Engine," CR 72677, 1970, NASA.

[4] Rawlin, V. K. and Kerslake, W., "Durability of the SERT II Hollow Cathode and Future Applications of Hollow Cathodes," *Journal of Spacecraft and Rockets*, Vol. 7, No. 1, Jan. 1970, pp. 14–20; also TMX 52532, 1969, NASA.

Ground and Flight Test Results for a Decelerator Towline Energy Absorber

Ross L. Goble* and Earl L. Councill Jr.†
NASA Langley Research Center, Hampton, Va.

EARLY flights in the Planetary Entry Parachute Program (PEPP) indicated a high shock peak and an oscillatory response of the payload during early phases of payload deceleration.[1,2] The oscillations appeared to be more severe at increased Mach numbers. Since an even higher Mach number ($M = 3.5$) was planned for the disk-gap-band parachute (Fig. 1) in the Supersonic High Altitude Planetary Experiment (SHAPE) program, it appeared that shock attenuation would be required. This Note presents the experimental effort associated with the design of the energy

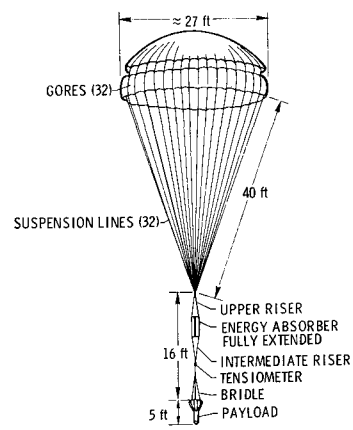

Fig. 1 Parachute dimensional details and flight configuration.

Presented as Paper 70-1202 at the AIAA Aerodynamic Deceleration Systems Conference, September 14–16, Dayton, Ohio; submitted October 8, 1970; revision received December 16, 1970.

* Aero-Space Technologist. Member AIAA.
† Aero-Space Technologist.